



Lawrence Berkeley Laboratory

UNIVERSITY OF CALIFORNIA

Submitted to Nuclear Physics A

Hot Nuclei in a Nucleon Vapor

G. Fai and J. Randrup

May 1988

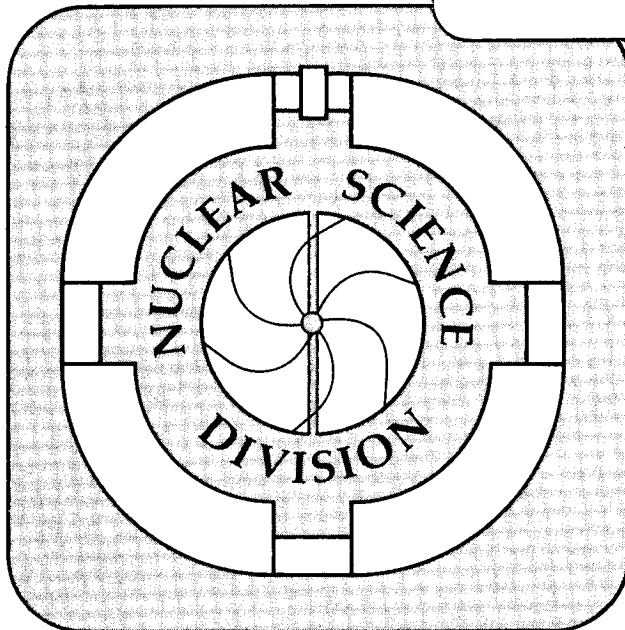
RECEIVED
LAWRENCE
BERKELEY LABORATORY

JUL 3 1988

LIBRARY AND
DOCUMENTS SECTION

TWO-WEEK LOAN COPY

*This is a Library Circulating Copy
which may be borrowed for two weeks.*



LBL-24845
c.2

DISCLAIMER

This document was prepared as an account of work sponsored by the United States Government. While this document is believed to contain correct information, neither the United States Government nor any agency thereof, nor the Regents of the University of California, nor any of their employees, makes any warranty, express or implied, or assumes any legal responsibility for the accuracy, completeness, or usefulness of any information, apparatus, product, or process disclosed, or represents that its use would not infringe privately owned rights. Reference herein to any specific commercial product, process, or service by its trade name, trademark, manufacturer, or otherwise, does not necessarily constitute or imply its endorsement, recommendation, or favoring by the United States Government or any agency thereof, or the Regents of the University of California. The views and opinions of authors expressed herein do not necessarily state or reflect those of the United States Government or any agency thereof or the Regents of the University of California.

Hot Nuclei in a Nucleon Vapor

*George Fai * and Jørgen Randrup*

Nuclear Science Division, Lawrence Berkeley Laboratory
University of California, Berkeley, California 94720

May 13, 1988

Abstract:

We consider excited nuclear matter at densities somewhat below the saturation density. The system is described in terms of excitable nuclear fragments embedded in a nucleon vapor. With a view towards applications to medium-energy nuclear collisions, we propose a specific factorization of the total partition function by which the individual quasifragments can be formally separated from the vapor: a given nucleon is considered part of a particular fragment to the extent that it is reflected back from the nuclear surface when attempting to leave the domain occupied by that fragment. This prescription leads to a mass-dependent limiting nuclear temperature. A number of other prescriptions used in the past are also examined and compared.

* On leave of absence from Department of Physics, Kent State University, Kent, Ohio 44242.

This work was supported by the Director, Office of Energy Research, Division of Nuclear Physics of the Office of High-Energy and Nuclear Physics of the U.S. Department of Energy under Contract DE-AC03-76SF00098 and under Grant DE-FG02-86ER40251.

1 Introduction

Statistical concepts play a central role in our understanding of the outcome of nuclear collisions. In low-energy collisions the transient systems formed evolve slowly and their excitation energy remains well below their binding energy, so that standard statistical evaporation models can be employed to describe the deexcitation process. As the energy is raised to medium energies, many-fragment final states grow abundant. Statistical methods are frequently applied in this regime to consider the production of several complex fragments. At still higher energies some simplicity is again achieved: the final states contain predominantly simple particles (nucleons and pions), and statistical “fireball” models can be utilized. This schematic summary serves to exhibit the fact that different scenarios prevail at different energies and that relative simplicity in the model description can be achieved when care is taken to identify the physically significant degrees of freedom.

Historically, the statistical description of nuclear collisions at medium energies evolved from phase-space calculations of exploding fireballs at relativistic energies [1,2]. Naturally, the primary degrees of freedom considered were those associated with the most abundantly produced simple particles, nucleons and pions, and the production of complex, excitable fragments was treated as a correction. Later on, the grand-canonical formulation was generalized to incorporate the simultaneous production of several complex and excitable fragments [3]. From the opposite starting point, Friedman and Lynch treated the disassembly of a hot nuclear source within the standard sequential-evaporation model developed for deexcitation processes at lower, relatively moderate temperatures [4]. The compound-nucleus aspects have also been emphasized by Moretto [5,6]. Nuclear collisions at medium and high energies are expected to exhibit both explosive and evaporative characteristics, due to the dynamical separation of the collision system into sources of qualitatively different degrees of excitation (“participants” and “spectators”). Therefore, to the extent that the high- and low-energy aspects of the process can be separated, one may apply either explosion or evaporation models to the appropriate parts of the problem [7,8].

The two opposite extremes, *explosion* at high energies and *evaporation* at low energies, should emerge as the appropriate limits of a more general statistical disassembly theory. Through the past several years, considerable progress has been made towards this goal, the most recent accomplishment being the formulation of a micro-canonical model for interacting fragments embedded in a nucleon vapor [9]. Although this model provides a well-founded formal framework for statistical studies of subsaturation nuclear matter, several specific ingredients remain to be improved before “realistic” calculations would be meaningful, including the interaction between the fragments, the dependence of their binding energy on temperature, isospin effects, and the formal separation of the fragments from the vapor. In the present work we address this latter problem. Thus, we focus our attention on subsaturation nuclear matter at medium energies (where the temperature is typically of the order of ten MeV). An important property of such systems is their tendency to form clusters and

it is natural to formulate a model in terms of such individual (but interacting) clusters. Accordingly, the most relevant variables are the masses, positions, and momenta of distinct *complex* fragments, together with their degree of intrinsic excitation, and the positions and momenta of individual vapor nucleons. We focus particularly on the description of a single such cluster, a *quasifragment*, embedded in a hot vapor of nucleons. Such a quasifragment can be regarded as a generalization of the concept of an ordinary atomic nucleus at low temperatures (where the coupling to the vapor is unimportant).

The quantitative importance of incorporating unstable excited states into statistical models for nuclear disassembly is brought out by experimental evidence indicating that metastable composite fragments are formed abundantly in nuclear collisions at medium energies [10,11]. In our previous treatment of nuclear disassembly [8], a particular unstable fragment state was included in the final phase space provided its (estimated) half-life exceeded the time characterizing the breakup process. A similar prescription was also employed in the exact microcanonical model of nuclear disassembly [9]. Although such life-time arguments are intuitively appealing in the context of a disassembling source, their relevance is less clear for the treatment of static problems, *e.g.* excited infinite nuclear matter at subsaturation densities. It is therefore desirable to seek a better foundation for the description of highly excited nuclear states, applicable to both static and dynamical scenarios. This is also practically important for the implementation of event generators developed to provide samples of multi-fragment final states of medium-energy nuclear collisions [12]. Furthermore, microscopic dynamical simulations (*e.g.* [13,14,15,16]) also encounter the problem when seeking to give a realistic description of the final nuclear fragments.

A consistent treatment of the metastable fragment states can only be achieved if a nucleon vapor is included in the calculation [9,17,18,19,20]. Therefore, we discuss a hot nucleus embedded in a vapor of nucleons. By the generalized Levinson's Theorem [21], the total partition function of the entire system is invariant to the partitioning of the levels between the nucleus and the vapor, in the independent-particle idealization. However, as mentioned above, in practice it is important to calculate the yields of different fragment types, and the final (post-evaporation) species distribution is sensitive to how this separation is made. The separation is also relevant to the question of the liquid-vapor phase transition in nuclear matter [22,23]. Similar questions were also discussed in the context of astrophysical applications [17,24] and in the framework of Hartree-Fock calculations [25].

In Section 2 we provide the formal background basis for our treatment of a hot nucleus embedded in a vapor of nucleons. Then, in Section 3, we study an individual quasifragment on the basis of the single-particle approximation. Starting from the Fermi-gas single-particle level density, we calculate the mean excitation energy (and its dispersion) of nuclei embedded in the vapor, as a function of the imposed temperature. We study different prescriptions for the inclusion of excited levels in the intrinsic partition function of the quasifragment and we obtain an effective nuclear temperature, facilitating comparisons with various previously employed prescriptions.

In Section 4 we study effective many-body level densities and the different approximations involved in deriving them. The Appendix treats a simple one-dimensional example exhibiting some characteristic features of the vapor-nucleus system.

2 Hot Subsaturating Nuclear Matter

Our present studies are directed towards nuclear matter at densities near (but below) the saturation density ($\approx 0.17 \text{ fm}^{-3}$) and at excitations comparable to the nuclear binding energy ($\approx 10 \text{ MeV}$ per nucleon). Under such circumstances, the system will typically appear as an assembly of clusters, *quasifragments*, interspersed with free nucleons, the *vapor*. For simplicity, we shall base our analysis below on the single-particle idealization, according to which the states of the many-body system can be generated by repeated excitation of individual particles. Note that in general the particles can be thought of as quasi-particles [26]. In this sense, the single-particle idealization is less restrictive than may appear at first sight.

The grand-canonical ensemble is well suited for the statistical description of nuclear fragments in equilibrium with a nucleon vapor. In the single-particle idealization, it is possible to express the total partition function Z in terms of the density of single-particle states, $g(\epsilon)$ [27],

$$\ln Z(\alpha, \beta) = \int g(\epsilon) \ln[1 + e^{-\alpha - \beta\epsilon}] d\epsilon . \quad (1)$$

Here β is the inverse of the imposed temperature τ and α is related to the chemical potential μ by $\alpha = -\beta\mu$.

The mean number of nucleons in the system and its mean energy are then given by

$$\langle A \rangle = -\frac{\partial \ln Z}{\partial \alpha} = \int \frac{g(\epsilon)}{1 + e^{\beta(\epsilon - \mu)}} d\epsilon , \quad (2)$$

$$\langle E \rangle = -\frac{\partial \ln Z}{\partial \beta} = \int \frac{g(\epsilon) \epsilon}{1 + e^{\beta(\epsilon - \mu)}} d\epsilon . \quad (3)$$

The requirement that the system contain a specified number of nucleons on the mean yields an implicit equation for the chemical potential $\mu(\tau)$, which can be readily solved by iteration. The second equation then yields the mean excitation energy per nucleon as a function of the imposed temperature τ . (The ground-state energy is obtained by evaluating (3) for $\tau = 0$.) It should be noted that this manner of calculating the energy of the system is only approximate, since in general the many-body energy is *not* the sum of individual-particle energies; the proper realm of applicability of the method is to relatively low-lying excitations, which can be considered as built of nearly independent (quasi)particle excitations.

2.1 General considerations

Before proceeding with our analysis of the multifragment situation, we wish to address briefly the relevance of Levinson's Theorem [21,28] in the framework of the

simpler scenario provided by a single nucleus embedded in the vapor of nucleons. In the Appendix, a further simplified situation is analyzed in greater detail. Let $g_0(\epsilon)$ be the density of single-particle states for a constant potential $V \equiv 0$, *i.e.* in the absence of fragments. Now introduce a potential well into the potential V and let the corresponding modified density of single-particle states be $g_V(\epsilon)$. We first note that the induced change can be written in the form

$$\Delta g(\epsilon) \equiv g_V(\epsilon) - g_0(\epsilon) = \sum_{\ell n} (2\ell + 1) \delta(\epsilon - \epsilon_{n\ell}) + \frac{1}{\pi} \sum_{\ell} (2\ell + 1) \frac{d\delta_{\ell}(\epsilon)}{d\epsilon}. \quad (4)$$

Here the first sum expresses the addition of the bound levels ($\epsilon_{n\ell} < 0$) of the well, each being characterized by its orbital angular momentum ℓ and its radial quantum number n . The second sum expresses the change in the density of unbound states in terms of the phase shifts $\delta_{\ell}(\epsilon)$. It should be noted that this latter term is negative for most values of the energy ϵ , since the phase shift exhibits an overall decrease as the energy is raised (in fact, $\delta_{\ell}(\epsilon) \rightarrow 0$ as $\epsilon \rightarrow \infty$). In particular, the total number of single-particle states remains unchanged by the modification of V ,

$$\Delta N \equiv \int \Delta g(\epsilon) d\epsilon = \sum_{\ell} (2\ell + 1) N_{\ell} + \frac{1}{\pi} \sum_{\ell} (2\ell + 1) (\delta_{\ell}(\infty) - \delta_{\ell}(0)) = 0. \quad (5)$$

This statement is a generalization of Levinson's Theorem [21,28], which was used in (5) in the form stating that the phase shift at zero energy equals π times the number of bound states, $\delta_{\ell}(0) = \pi N_{\ell}$ [29].

A key issue in the present study is how to partition the single-particle states between the quasifragment and the vapor. For the discussion of this problem it is useful to adopt a semiclassical picture in which any single-particle state can be associated with definite regions of space. The modification in the effective single-particle potential V , the formation of the nuclear potential well, is confined to near the domain occupied by the nuclear fragment, $\Omega_A \approx \frac{4\pi}{3} R_A^3$, and leaves the environment unchanged. The same must be the case for the associated single-particle states. If the dependence of $g(\epsilon)$ on the total volume Ω is known, it is easy to express the contribution $g_{>}(\epsilon)$ from nucleons located outside the fragment domain,

$$g_{>}(\epsilon) = \bar{\Omega} \frac{dg_V(\epsilon)}{d\Omega} = \bar{\Omega} \frac{dg_0(\epsilon)}{d\Omega}, \quad (6)$$

where $\bar{\Omega} = \Omega - \Omega_A$. While it appears reasonable to associate these states with the vapor, the classification of nucleons situated within the domain occupied by the fragment is less clear. At the low-energy end it is obvious that the bound levels are associated with the fragment. Conversely, at the highest energies, where the presence of the potential well is barely discernible, it appears most reasonable to associate the states with the vapor. There is probably no unique way to resolve this problem and the specific criterion we have adopted is based on physical arguments.

One might at first be tempted to identify the change $\Delta g(\epsilon)$ in (4) as the density of single-particle states associated with the quasifragment. However, this suggestion

appears somewhat unphysical, considering the fact exhibited above (see eq. (5)) that the contribution of $\Delta g(\epsilon)$ to ΔN is negative for $\epsilon > 0$.

A more attractive (yet simple) possibility is to associate the bound single-particle levels $\epsilon_{n\ell}$ with the fragment and let the second term in (4) represent the compensating depletion of the vapor states. This amounts to saying that the quasifragment is built out of all many-body states with bound single-particle excitations. (This prescription leads to the “cool” limit considered in some detail in Section 3.) Such many-body states are expected to be fairly long-lived, since residual configuration mixing is required to promote a single nucleon to an unbound orbital from which it may escape.

However, as has been clear since the general understanding of the compound nucleus was achieved, even unbound nucleon orbitals may have considerable longevity due to their quantal reflection from the nuclear surface [30]. (This is demonstrated *e.g.* by a recent experiment [11], observing the decay of the ground state of ${}^5\text{Li}$ into a proton plus an α -particle.) It is with this feature in mind that we propose that the many-body states to be associated with the nucleus are those generated by metastable single-particle orbitals, the degree of metastability being determined by the associated reflection coefficient (see Section 3.2 for details).

2.2 Identification of the nuclear level density

Let us now consider a system of several (non-overlapping) quasifragments immersed in a nucleon vapor, such as hot nuclear matter at subsaturation densities is expected to typically appear. As an approximation to an infinite system, let us impose periodic boundary conditions and confine our considerations to the volume Ω of an elementary cell. If no fragments are present, the effective single-particle potential is constant and the corresponding density of single-particle states, $g_0(\epsilon)$, is that of a Fermi-Dirac gas of nucleons. The presence of quasifragments in the system is felt by the individual nucleons as a modification of the effective single-particle Hamiltonian in the domains of the fragments (roughly speaking, each fragment generates its own potential well). The induced change in the density of single-particle states is $\Delta g(\epsilon) = g(\epsilon) - g_0(\epsilon)$. (In the case of a single quasifragment $\Delta g(\epsilon)$ is given by (4).)

To the extent that the fragments do not overlap, the change $\Delta g(\epsilon)$ can be decomposed uniquely into contributions from the N individual quasifragments,

$$g(\epsilon) = g_0(\epsilon) + \Delta g(\epsilon) = g_0(\epsilon) + \sum_{n=1}^N \Delta g_n(\epsilon) . \quad (7)$$

Here $\Delta g_n(\epsilon)$ is the change effected by the introduction of fragment number n and it can be written in the form

$$\Delta g_n(\epsilon) \approx g_n(\epsilon) - \Omega_n \frac{\partial}{\partial \Omega} g_0(\epsilon) . \quad (8)$$

The first term, $g_n(\epsilon)$, is the density of single-particle states associated with the fragment n when its potential well is artificially extended upwards so that no continuum

states occur. The second term subtracts the part of the original level density $g_0(\epsilon)$ stemming from single-particle states located within the domain of the fragment, Ω_n . The precise definition of the fragment volumes is of course somewhat uncertain, but since the total partition function Z is independent of the definition of Ω_n , this uncertainty is expected to have little practical importance; we shall use $\Omega_n = \frac{4\pi}{3}R_n^3$, where R_n is the equivalent sharp radius of a nucleus with the mass number A_n .

As mentioned earlier, the level density $g_n(\epsilon)$ must be split so that only its lower-energy part $\tilde{g}_n(\epsilon)$ is to be associated with the fragment while its higher-energy part $\bar{g}_n(\epsilon)$ should be associated with the vapor. This separation is made in the present work by invoking the average reflection and transmission coefficients for single-particle states at a given energy, $\bar{R}_n(\epsilon)$ and $\bar{T}_n(\epsilon)$ (see Section 3 for details),

$$g_n(\epsilon) = g_n(\epsilon)\bar{R}_n(\epsilon) + g_n(\epsilon)\bar{T}_n(\epsilon) = \tilde{g}_n(\epsilon) + \bar{g}_n(\epsilon) . \quad (9)$$

Thus, in summary, the density of single-particle states for the total system is decomposed as follows,

$$g(\epsilon) = g_{\text{vapor}}(\epsilon) + \sum_{n=1}^N \tilde{g}_n(\epsilon) , \quad (10)$$

where the part associated with the nucleon vapor is

$$g_{\text{vapor}}(\epsilon) = \bar{\Omega} \frac{\partial}{\partial \Omega} g(\epsilon) + \sum_{n=1}^N \bar{g}_n(\epsilon) , \quad (11)$$

with $\bar{\Omega} = \Omega - \sum_n \Omega_n$ being the volume outside of the N fragments.

The partition function Z for the total system then factorizes correspondingly, $Z = Z_{\text{vapor}} \prod_{n=1}^N \tilde{Z}_n$, where

$$\ln \tilde{Z}_n = \int \tilde{g}_n(\epsilon) \ln[1 + e^{-\alpha - \beta\epsilon}] d\epsilon \quad (12)$$

is the intrinsic partition function associated with fragment n and Z_{vapor} is given analogously in terms of $g_{\text{vapor}}(\epsilon)$. It should be noted that the total partition function Z is independent of the particular way in which the partition of $g_n(\epsilon)$ is made (as is evident from (1)), as long as the single-particle idealization is maintained. It might therefore seem unnecessary to make that partition. However, the partition of $g_n(\epsilon)$ is important in two respects:

- 1) The single-particle idealization is only an approximation and ignores many-body aspects responsible for the fragment formation. In previous treatments of the nucleus-vapor problem the fragment itself has been included only as a modification of the mean field, whereas we are attempting to include it dynamically by way of incorporating its overall motion as a degree of freedom. Whether a nucleon moving in the domain of the quasifragment should be considered part of that fragment depends on to what extent it is likely to share its momentum with the fragment, and this property is closely related to its reflection coefficient: if it is reflected back into the interior it is more likely to ultimately equilibrate with the fragment whereas its

ready transmission will leave the fragment rather unaffected. It is also important to recall that the potential well representing the fragments arises from the nucleonic interaction itself, and the corresponding overcounting of degrees of freedom needs to be corrected for in a more refined treatment.

2) Our motivation for studying subsaturation nuclear matter is the insight it may give into the nuclear disassembly processes occurring in the course of medium-energy nuclear collisions. In this context the properties of idealized infinite matter at equilibrium are related to the explosive break-up by means of a transition-state assumption, so that the idealized results are assumed to describe the finite nuclear source at its freeze-out stage. Subsequent to this stage, the primary highly excited quasifragments will undergo sequential decay processes which generally decrease their mass and charge. This effect is known to be quantitatively important and depends on the degree of excitation of the quasifragments, a property directly related to $\tilde{g}_n(\epsilon)$. Thus, for the practical applications of our model it is essential to address the problem of how to partition the level density between vapor and fragment(s).

3 Single-Particle Level Densities

In this Section we consider a single quasifragment. Its mean mass is A and its density of single-particle states is $\tilde{g}_A(\epsilon)$, from which the fragment's partition function \tilde{Z}_A can be calculated according to eq. (12). The excitation spectrum of the quasifragment can be characterized in terms of a moment expansion. Most significant is the mean excitation energy per nucleon in the fragment,

$$\mathcal{E} = \frac{1}{A_0}(\langle E \rangle - E_0). \quad (13)$$

Here $\langle E \rangle = -\partial \ln \tilde{Z}_A / \partial \beta$ is the mean energy and E_0 is the mean energy for $\tau = 0$. A convenient measure of the dispersion of the distribution around the mean value is given by

$$\left[\frac{\sigma_E^2}{A} \right]_{A=A_0} = \left[A \sigma_{\mathcal{E}}^2 \right]_{A=A_0} = \frac{1}{A_0} \left(\sigma_{EE} - \frac{\sigma_{AE} \sigma_{EA}}{\sigma_{AA}} \right). \quad (14)$$

Here the covariance between A and E is given by $\sigma_{AE} = \partial^2 \ln \tilde{Z}_A / \partial \alpha \partial \beta$ and the variances $\sigma_A^2 = \sigma_{AA}$ and $\sigma_E^2 = \sigma_{EE}$ are given analogously. The quantity in (14) is the variance in energy for a fixed mass number. Accordingly, the spurious contribution to the energy variance arising from the grand-canonical fluctuation in mass number has been subtracted (last term on the right). The division by A_0 is made for convenience and ensures that the quantity becomes a constant in the macroscopic limit, just as \mathcal{E} does.

We will now investigate how different physical assumptions affect the mean excitation energy of the fragment (13) and its reduced variance (14).

3.1 Limits and phenomenological formulae

As a starting point, we consider the Fermi-gas single-particle level density:

$$g_{\text{hot}}(\epsilon) = \frac{3A}{2T_F} \left(\frac{\epsilon - V}{T_F} \right)^{\frac{1}{2}} = \frac{3A}{2T_F} \left(\frac{\epsilon^*}{T_F} \right)^{\frac{1}{2}} = A\hat{g}_{\text{hot}}(\epsilon), \quad (15)$$

where $T_F \approx 37$ MeV is the Fermi kinetic energy and $V \approx -45$ MeV is the value of the constant potential in the nuclear interior. For later convenience, the single-particle energy relative to the bottom of the well, $\epsilon^* = \epsilon - V$, has been introduced. In the rightmost equation we have exhibited the simple A -dependence of the Fermi-gas single-particle level density. The use of the reduced level density $\hat{g}(\epsilon)$ makes the results independent of the mass number of the fragment, when surface effects are neglected. (This simple scaling law will be broken by introducing a mass-dependent definition of the fraction of single-particle levels that should be associated with the nucleus, as is the case when the average reflection coefficient suggested in Section 2 is used.) The Fermi-gas level density (15) describes an idealized scenario in which the fragment is surrounded by an infinitely high potential wall (isolated nucleus). Thus, the escape of nucleons into the vapor is disregarded and the maximum possible amount of excitation energy is stored in the nucleus. Therefore, we will denote this extreme situation the “hot” limit.

Another natural reference situation is the ‘cool’ scenario, mentioned in Section 2.1, in which any unbound single-particle state is part of the vapor so that the many-body states associated with the quasifragment are those built out of bound single-particle states,

$$\hat{g}_{\text{cool}}(\epsilon) = \frac{3}{2T_F} \left(\frac{\epsilon - V}{T_F} \right)^{\frac{1}{2}} \theta(-\epsilon). \quad (16)$$

The truncation function θ guarantees that only levels with $\epsilon < 0$ contribute to the quasifragment. It should be recognized that this “cool” scenario accomodates quite highly excited nuclei by traditional standards, since excitations as high as ≈ 8 MeV per nucleon can be built from bound single-particle states. (A more truly ‘cold’ situation would arise if only bound *many*-body states were incorporated, as in the original discussion of nuclear disassembly [3]).

The physical situation of present interest is expected to be bracketed by the above two limits, since some fragments will be produced with one or more individual particles excited above the separation energy [24]. Several approximate methods can be used to represent this scenario. We will first examine several phenomenological prescriptions for truncating the *single*-particle level density, in analogy with prescriptions used in the literature to truncate the *many*-particle level densities (see Section 4). We focus particularly on prescriptions using an exponential cutoff,

$$\hat{g}_{\text{exp}}^{\text{eff}}(\epsilon) = \frac{3}{2T_F} \left(\frac{\epsilon^*}{T_F} \right)^{\frac{1}{2}} e^{-\epsilon/\tau_0} \theta(-\epsilon), \quad (17)$$

or a Gaussian cutoff,

$$\hat{g}_{\text{Gauss}}^{\text{eff}}(\epsilon) = \frac{3}{2T_F} \left(\frac{\epsilon^*}{T_F} \right)^{\frac{1}{2}} e^{-\epsilon^2/2\tau_0^2} \theta(-\epsilon). \quad (18)$$

In both (17) and (18), the cutoff-parameter τ_0 is the width of the modulation function.

As a function of the imposed temperature τ , fig. 1 displays the mean excitation energy per nucleon, \mathcal{E} , as given by (13), and the square root of the reduced variance (14), for the hot and cool scenarios as well as the above two phenomenological prescriptions. It can be seen from the figure that the exponential and Gaussian cutoffs are approximately equivalent with each other, although the ‘Gaussian’ curves lie somewhat above the ‘exponential’ ones for the temperatures considered. Figure 1 offers a convenient possibility for introducing an effective intrinsic nuclear temperature τ_{eff} . This quantity can be defined as that temperature for which the mean excitation energy, as calculated in the hot scenario, comes out the same as that arrived at when using the truncated level density at the actual temperature: $\mathcal{E}(g_{\text{hot}}, \tau_{\text{eff}}) = \mathcal{E}(g_{\text{eff}}, \tau)$. Since $g_{\text{hot}} > g_{\text{eff}}$, the effective temperature τ_{eff} is always smaller than the imposed temperature τ , and it approaches τ_0 when $\tau \gg \tau_0$. Thus, as discussed in Ref. [9], τ_0 can be interpreted as a *limiting* temperature, the maximum temperature attainable by the excited nucleus. Hartree-Fock calculations at finite temperature are known to exhibit a limiting temperature [31]. In Fig. 1. we show results with $\tau_0 = 100$ MeV to demonstrate the convergence to the hot scenario, and with $\tau_0 = 12$ MeV, chosen as an illustrative value for the expected limiting temperature.

3.2 Cutoff with the reflection coefficient

In this Section, we develop a ‘parameter-free’ approximate method for defining an appropriate effective single-particle level density. For this, we utilize the quantum-mechanical reflection coefficient for a nucleon in a given single-particle orbital and demand that a given orbital be classified as belonging to the fragment with a probability equal to its associated reflection coefficient.

In order to estimate the reflection coefficient, we use the parabolic approximation near the top of the effective nuclear potential

$$V_{\text{eff}}(r) = -\frac{V_0}{1 + e^{(r-C_V)/d}} + \frac{\hbar^2}{2mr^2} \left(\ell + \frac{1}{2} \right)^2. \quad (19)$$

Here we have employed the usual WKB replacement, $\ell(\ell+1) \rightarrow (\ell + \frac{1}{2})^2$ [32]. Furthermore, $C_V \approx R_V (1 - (b_V/R_V)^2)$ is the central potential radius with $b_V \approx 1.2$ fm for the diffuseness of the potential. For the potential radius R_V we use $R_V = R_\rho + s - d/R_\rho$, where $R_\rho = r_0 A^{1/3}$ and we employ the parameter values $r_0 = 1.15$ fm, $s = 0.82$ fm, and $d = 0.56$ fm² [33].

The transmission coefficient of the ℓ^{th} partial wave can be expressed in the parabolic approximation as [34]

$$T_\ell(\epsilon) = \frac{1}{1 + e^{-2\pi\epsilon_\ell}}, \quad (20)$$

where the relative energy in excess of the barrier is

$$e_\ell = \frac{\epsilon - V_{\text{eff}}(r_{\text{top}}^\ell)}{\hbar\omega_\ell}, \quad (21)$$

with the characteristic frequency ω_ℓ determined by

$$m\omega_\ell^2 = -\frac{d^2V_{\text{eff}}}{dr^2}(r_{\text{top}}^\ell). \quad (22)$$

In eqs. (21) and (22) r_{top}^ℓ denotes the location of the maximum of the effective radial potential for the ℓ^{th} partial wave. With $R_\ell = 1 - T_\ell$, the average reflection coefficient for orbitals near a given energy ϵ is then given by

$$\bar{R}(\epsilon) = \frac{\sum_{\ell=0}^{\ell_{\text{max}}} (2\ell + 1) R_\ell(\epsilon)}{\sum_{\ell=0}^{\ell_{\text{max}}} (2\ell + 1)}, \quad (23)$$

where ℓ_{max} is the maximum value of angular momentum for which the effective potential has a minimum. The ensuing effective single-particle level density is then

$$\hat{g}_{\text{R}}^{\text{eff}}(\epsilon) = \frac{3}{2T_{\text{F}}} \left(\frac{\epsilon - V}{T_{\text{F}}} \right)^{\frac{1}{2}} \bar{R}(\epsilon). \quad (24)$$

Figure 2 shows the mean excitation energy per nucleon as calculated using the effective level density (24) for mass numbers $A = 40$ (dashed line) and for $A = 100$ (dots). For comparison we include the hot and cool scenarios and the results obtained with an exponential cutoff with $\tau_0 = 12$ MeV. The truncation in terms of the reflection coefficient introduces a natural A -dependence: a larger nucleus (having a smaller surface-to-volume ratio) holds more energy per nucleon at a given temperature, until this behavior saturates in the limit $A \rightarrow \infty$. For heavier nuclei, the limiting temperature is 10–12 MeV, while the limiting temperature comes out to be around 8 MeV for the lighter nuclei, which are relatively abundant in the scenarios of interest. Thus, for practical applications the reflection-coefficient prescription can be well approximated by *e.g.* an exponential cutoff with $\tau_0 \approx 8$ MeV. These values are roughly consistent with the limiting temperatures obtained in Hartree-Fock calculations [25], where mostly heavier nuclei are considered. Observe, however, that the limiting temperature is decreasing as a function of the mass number in the calculation of ref. [25].

4 Many-Body Level Densities

In this Section the mean excitation energy and its dispersion will be calculated starting from various *many-body* level densities. The many-body level density $\rho(A, E^*)$ can be obtained from the partition function by way of an inverse Laplace transformation [27]. For a given $\rho(A, E^*)$, it is useful to define the following moments,

$$\mathcal{I}_p = \int (E^*)^p \rho(A, E^*) e^{-\beta E^*} dE^*, \quad (25)$$

where $p=0, 1, 2$. These moments can be evaluated approximately by the stationary-phase method, which yields the equations

$$\left[\frac{\partial \ln \rho(A, E^*)}{\partial E^*} \right]_{E^*=E_p^*} + \frac{p}{E_p^*} = \beta \quad (26)$$

for the saddle-point energies E_p^* . We note that the partition function is given by $Z = \mathcal{I}_0$. Moreover, the mean excitation energy is $\langle E^* \rangle = \mathcal{I}_1/\mathcal{I}_0$ and its variance is $\sigma_{E^*}^2 = \mathcal{I}_2/\mathcal{I}_0 - \langle E^* \rangle^2$. These quantities have also been calculated by direct numerical integration. In addition, we developed a semi-analytic approximation along the lines of ref. [27], and compared the results to the ones obtained in the saddle-point approximation. Although these methods improve somewhat on the results obtained in the saddle-point approximation (particularly at lower temperatures), in the following we present the saddle-point results, due to their clarity. The other approximations developed have been used to check the results of the saddle-point calculations.

4.1 Fermi-gas level density

Using the saddle-point approximation in calculating $\rho(A, E^*)$, Bohr and Mottelson [27] obtain for the many-body level density

$$\rho(A, E^*) = \frac{1}{\sqrt{48E^*}} e^{2[\frac{\pi^2}{6} g_A (V+T_F) E^*]^{\frac{1}{2}}} = \frac{1}{\sqrt{48E^*}} e^{2[\frac{\pi^2}{6} \frac{3A}{2T_F} E^*]^{\frac{1}{2}}}, \quad (27)$$

where in the rightmost equation it has been used that the density of single-particle states in a Fermi gas is given by $g_A(T_F) = 3A/2T_F$ at the Fermi surface (see eq. (15)).

It is customary to express the exponent in (27) in the form $2(a_A E^*)^{1/2}$ with the level-density parameter

$$a_A = \frac{\pi^2}{6} \frac{3A}{2T_F} = \frac{A}{e_0}. \quad (28)$$

For the nuclear Fermi gas, $e_0 = 4T_F/\pi^2 \approx 16$ MeV, whereas for finite nuclei a smaller value, $e_0 \approx 8-10$ MeV, is required to reproduce the available experimental information [35]. The level-density parameter (28) is derived for a single-particle gas in a sharp-surface potential well. The effect of the nuclear surface diffuseness is significant and accounts to a large degree for the observed values [36]. In addition, correlation effects play an important role [37]. Although the level-density parameter can be considered temperature dependent [38], we adopt the standard form (28) for simplicity.

It is straightforward to calculate the mean excitation energy per nucleon and its reduced dispersion from the level density (27) in the saddle-point approximation (26). These quantities are shown in Fig. 3 as a function of the temperature for $A = 20, 40$ and 100 (dots, short dashes and long dashes, respectively), together with the results of the full calculation ((13) and (14)) with the ‘hot’ single-particle level density (15). It should be noted that the formal applicability of the saddle-point approximation

requires $A > 4e_0/\tau$. We see from Fig. 3 that the standard approximation (27) is appropriate for sufficiently heavy systems in the temperature range $2 \text{ MeV} < \tau < 10 \text{ MeV}$. For higher temperatures the saddle-point approximation overestimates the mean excitation energy and its dispersion. For smaller systems the approximation (in particular for the dispersion) breaks down at low temperatures.

4.2 FREESCO level density

Based on the realization that the essential energy-dependence of the level density (for sufficiently high energies) comes through the exponential in (27), the simpler expression without the preexponential energy dependence,

$$\rho(A, E^*) = C e^{2(a_A E^*)^{1/2}}, \quad (29)$$

is also frequently used in practice [35]. This form has the additional advantage of being well-behaved at very low excitations. Alternatively, the singularity of the level density (27) can be removed analytically by subtracting the ground-state contribution before using the saddle-point approximation [39]. We will now use the simple expression (29) for the calculation of the moments (25). The value of the constant C is immaterial for this purpose.

To account for the large surface-to-volume ratio of the light nuclei, the simplified level density (29) was further modified in ref. [7], where a surface correction to the level-density parameter (28) was introduced. In the standard version of the *FREESCO* event generator [12] the modified many-body level density

$$\begin{aligned} \rho(A, E^*) &= k_1 A^{-p} e^{2\sqrt{a_A E^*}}, \\ a_A &= (1 - k_2 A^{-\frac{1}{3}}) \frac{A}{e_0}, \end{aligned} \quad (30)$$

is employed with the parameter values $k_1 = 0.2 \text{ MeV}^{-1}$, $p = \frac{5}{3}$, $k_2 = 0.8$, and $e_0 = 8 \text{ MeV}$. Although these parameters have been adjusted to reproduce available data on light nuclei, the formula (30) is expected to be only a crude approximation.

We now examine the approximations (29) and (30), treating e_0 as an adjustable parameter. Figure 4 displays the mean excitation energy per nucleon calculated with the level densities (29) and (30) in the saddle-point approximation. Short dashes and long dashes represent the result of the calculation using (29) with $e_0 = 8, 16 \text{ MeV}$, respectively. Alternating long-short dashes and the dotted line correspond to (30) with $e_0 = 8, 16 \text{ MeV}$, respectively. It is seen that (30) with $e_0 = 16 \text{ MeV}$ yields the best reproduction of the results of the full calculation based on the Fermi-gas single-particle level density (solid line). (Note that in actual applications all of these many-body level densities will be modulated with a truncation factor, as discussed in Section 3.)

The level density (30) with $e_0 = 8 \text{ MeV}$, as used in *FREESCO*, seriously overestimates the mean excitation energy and its dispersion at temperatures of 10-15 MeV. Some of this overestimation can be compensated for by the cutoff procedure.

However, (30) with $e_0 = 8$ MeV remains unsatisfactory for two reasons: (i) the level-density parameter should approach that of a Fermi gas when $A \rightarrow \infty$, and (ii) as demonstrated on the basis of the leptodermous expansion in ref. [36], the presence of the nuclear surface is expected to increase (rather than decrease) the density of many-body levels.

Motivated by the above shortcomings, we have developed an improved version of the *FREESCO* level density based on ref. [36]. The simplest semi-empirical formula with surface correction in ref. [36] suggests the values $e_0 = 14.61$ MeV and $k_2 = -4$ in (30) for spherical nuclei. The mean excitation energy per nucleon obtained with this prescription for $A = 40$ is displayed by the alternating long-short dashes in Fig. 5. We show the results of the full calculation based on the single-particle level density (solid line), and the many-body calculations with $e_0 = 16$ MeV in the form (29) (long dashes) and in the *FREESCO* level density (30) (dotted line) for comparison. We see that the simple semi-empirical formula of [36] with its original parameters overestimates the mean excitation energy and its dispersion. Adjusting the parameters to $e_0 = 16$ MeV and $k_2 = -1$ (short dashes) brings the results closer to the results of other models. This prescription then has the proper limit as $A \rightarrow \infty$ and the desired behaviour of the surface correction.

4.3 Effective many-body level densities

As we have seen in Section 3, both an exponential and a Gaussian cutoff provide fairly good representations of the effective single-particle level density obtained by modulating with the average reflection coefficient $\bar{R}(\epsilon)$. A Gaussian modulation factor is used on the many-body level densities in the standard version of *FREESCO*, while an exponential cutoff was introduced in ref. [9]. In this section we compare these two prescriptions within the framework of the event generator.

Figure 6 displays a histogram of the total mean excitation energy in a quasifragment as a function of its mass number, as distributed after the first grand-canonical iteration in *FREESCO* (see ref. [8] for details). The different prescriptions for the modulating factor are denoted by different degree of shading of the vertical bars. As in the standard version of *FREESCO* [12], the lower states of the fragments are explicitly included in the calculation. (In particular, note the excited state of ${}^4\text{He}$ at 20.3 MeV.) For higher excitations, where the experimental information is scarce, we use the level density (30), appropriately modulated by a truncation factor. The bar in the foreground of fig. 6 represents the Gaussian cutoff used in *FREESCO*:

$$\rho^{\text{eff}}(A, E^*) = \rho(A, E^*) e^{-(E^*-B)^2/2\tau_0^2} \theta(B - E^*) , \quad (31)$$

with the level density as in (27), B being the lowest barrier against light-particle emission, and a mass-dependent cutoff parametrized as $\tau_0 = 8(\sqrt{A-3} - 1)$ MeV for mass numbers $A > 4$. The second and third bars in Fig. 6 correspond to a simple exponential cutoff,

$$\rho^{\text{eff}}(A, E^*) = \rho(A, E^*) e^{-(E^*-B)/\tau_0} \theta(B - E^*) , \quad (32)$$

with $\tau_0 = 8, 16$ MeV, respectively. We conclude from this figure that a limiting temperature of 8 MeV provides a better representation of the results obtained with the Gaussian cutoff. It may be even more physically acceptable to introduce a mass-dependence of the limiting temperature in (32). We do not develop such an approximation in the present paper due to the arbitrariness associated with the procedure.

5 Concluding Remarks

In the present paper, we have addressed the description of hot subsaturation nuclear matter, such as may be produced in nuclear collisions at medium energies. The statistical treatment of such systems is conveniently formulated in terms of excitable quasifragments embedded in a nucleon vapor. At the high temperatures of interest, for which the excitation of the system is comparable to its binding energy, the metastable fragments must be considered in conjunction with a surrounding nucleon vapor. (Although this problem is well known from astrophysically motivated studies, the astrophysical temperatures and densities are considerably lower.)

We have formulated a parameter-free method for making a formal split of the partition function into a factor associated with the vapor and one factor for each quasifragment. This method can be characterized roughly by saying that a particular nucleon, situated within the interior of a fragment, is considered as part of that fragment if it is reflected back into the fragment's interior when reaching its surface. This prescription yields a mass-dependent limiting nuclear temperature, decreasing from 10–12 MeV for heavy nuclei to around 8 MeV for $A \approx 10$. Various other, commonly employed prescriptions for treating a single quasifragment have also been studied and compared.

The present study seeks to clarify certain aspects of the multifragmentation problem. Other, related aspects, for example the temperature dependence of the nuclear binding energy and the interaction between the quasifragments, also need to be clarified before a satisfactory multifragment model is at hand [23]. Moreover, it should be kept in mind that statistical considerations have to be augmented with more dynamical models (*e.g.* with respect to instabilities in hot nuclear matter [40], or about the time-dependence of the nuclear temperature [41]) in order to provide a more comprehensive description of medium-energy nuclear collisions.

We wish to acknowledge instructive discussions with P. Bonche, S.E. Koonin, S. Pratt, and P.J. Siemens. This work was supported by the Director, Office of Energy Research, Division of Nuclear Physics of the Office of High-Energy and Nuclear Physics of the U.S. Department of Energy under Contract DE-AC03-76SF00098 and Grant DE-FG02-86ER40251.

Appendix: Schematic analysis of s-wave scattering

In this Appendix we analyze a schematic model in order to illustrate our discussion in the main body of the text. We consider s-wave scattering from a finite, spherical square well inside which the potential has the value $V < 0$. The sharp well has the radius R and the entire system is enclosed in a larger sphere of radius R_0 . Due to the spherical symmetry, the problem effectively reduces to one dimension. Below we shall analyze this problem by semiclassical means.

For a particle with a given positive energy $\epsilon > 0$, the local wave number follows from energy conservation,

$$\epsilon = \frac{\hbar^2}{2m} k_0^2 = \frac{\hbar^2}{2m} k^2 + V, \quad (1)$$

where k is the wave number inside the well ($r < R$) and k_0 is the wave number outside ($r > R$). We note that the above relation implies $dk/dk_0 = k_0/k$. The eigenstates in the system are determined by the demand that the phase change from the origin to the outer boundary be an integer multiple of π ,

$$k_0(R_0 - R) + kR = N\pi. \quad (2)$$

From this relation the density of states can readily be obtained,

$$g(\epsilon) = \frac{dN}{d\epsilon} = \frac{m}{\pi\hbar^2} \left(\frac{R_0 - R}{k_0} + \frac{R}{k} \right). \quad (3)$$

In the absence of a well, corresponding to $V \equiv 0$, the density of states is given by $g_0(\epsilon) = (m/\pi\hbar^2)(R_0/k_0)$. Consequently, the change in level density caused by the introduction of the potential well is given by

$$\Delta g(\epsilon) \equiv g(\epsilon) - g_0(\epsilon) = -\frac{m}{\pi\hbar^2} \left(\frac{1}{k_0} - \frac{1}{k} \right) R = \frac{1}{\pi} \frac{d}{d\epsilon} \delta(\epsilon). \quad (4)$$

In the last relation we have introduced the phase shift

$$\delta(\epsilon) = [k_0(R_0 - R) + kR] - k_0R_0 = (k - k_0)R, \quad (5)$$

which is independent of R_0 . We note that $\delta(\epsilon) > 0$, whereas $d\delta(\epsilon)/d\epsilon < 0$.

A wave function for a given single-particle orbital is of the form

$$\begin{aligned} \psi(r < R) &= a\sqrt{2} \sin(kr) \\ \psi(r > R) &= a_0\sqrt{2} \sin(k_0r + \delta(\epsilon)) \end{aligned} \quad (6)$$

For our present semiclassical analysis it is more convenient to think of the wave functions as plane waves. The local amplitudes a and a_0 are determined by the requirements of normalization and continuity (*i.e.* the current density is conserved),

$$(R_0 - R)a_0^2 + Ra^2 = 1, \quad (7)$$

$$a_0^2 k_0 = a^2 k, \quad (8)$$

respectively. The local density of particles is then

$$\rho(r < R) = \sum_n f_n a^2 + \sum_{n < 0} f_n \frac{1}{R} = \sum_n f_n \frac{k_0}{(R_0 - R)k + Rk_0} + \frac{1}{R} \sum_{n < 0} f_n, \quad (9)$$

$$\rho(r > R) = \sum_n f_n a_0^2 = \sum_n f_n \frac{k}{(R_0 - R)k + Rk_0}. \quad (10)$$

Here f_n is the occupancy of a particular orbital n , and for $r < R$ we have included the contribution from the bound states (enumerated by negative values of n for convenience). If the single-particle orbitals are filled up to a specified (Fermi) energy $\epsilon_F = (\hbar^2/2m)k_F^2 > 0$, we have

$$\begin{aligned} \rho(r > R) &= \int_0^{\epsilon_F} d\epsilon g(\epsilon) a_0^2 = \frac{1}{\pi} \int_0^{k_F} dk_0 \left[1 - \frac{R}{R_0} \left(1 - \frac{k_0}{k}\right)\right] \left[1 - \frac{R}{R_0} \left(1 - \frac{k_0}{k}\right)\right]^{-1} \\ &= \frac{1}{\pi} \int_0^{k_F} dk_0 = \frac{k_F}{\pi} = \rho_0, \end{aligned} \quad (11)$$

where ρ_0 is the density for $V = 0$,

$$\rho_0 = \int_0^{\epsilon_F} d\epsilon g_0(\epsilon) \frac{1}{R_0} = \frac{1}{\pi} \int_0^{k_F} dk_0 = \frac{k_F}{\pi}. \quad (12)$$

Thus the density outside the potential well is unaffected by the introduction of the well, as intuition would suggest. The density within the domain of the well can be calculated in a similar manner,

$$\begin{aligned} \rho(r < R) &= \int_0^{\epsilon_F} d\epsilon g(\epsilon) a^2 + \frac{N_0}{R} \\ &= \frac{1}{\pi} \int_0^{k_F} dk_0 \left[1 - \frac{R}{R_0} \left(1 - \frac{k_0}{k}\right)\right] \frac{k_0}{k} \left[1 - \frac{R}{R_0} \left(1 - \frac{k_0}{k}\right)\right]^{-1} + \frac{N_0}{R} \\ &= \frac{1}{\pi} \int_0^{k_F} dk_0 \frac{k_0}{k} + \frac{N_0}{R} = \frac{1}{\pi} \int_{k_-}^{k_+} dk + \frac{N_0}{R} = \frac{k_+ - k_-}{\pi} + \frac{k_-}{\pi} = \frac{k_+}{\pi} = \rho_V. \end{aligned} \quad (13)$$

Here, in the last line we have introduced the local wave number k_- for a particle at zero energy, $\frac{\hbar^2}{2m}k_-^2 + V = 0$, and used that the number of bound states, N_0 , is determined by the condition $k_-R = N_0\pi$. Thus, the level density inside the domain of the well is equal to that of a Fermi gas in a constant potential of depth V , as one would expect.

In a semiclassical picture, the single-particle states can be considered as localized in phase-space. The contribution to level density $g(\epsilon)$ from elementary states located outside the well is given by

$$g_{>}(\epsilon) = (R_0 - R) \frac{\partial}{\partial R_0} g(\epsilon) = (R_0 - R) \frac{\partial}{\partial R_0} g_0(\epsilon) = \frac{R_0 - R}{R_0} g_0(\epsilon) = \frac{m}{\pi \hbar^2} \frac{R_0 - R}{k_0}. \quad (14)$$

These states should all be considered as part of the vapor. The remaining part is

$$g_{<}(\epsilon) = g(\epsilon) - g_{>}(\epsilon) = \frac{m}{\pi \hbar^2} \frac{R}{k}. \quad (15)$$

It can be split into contributions from single-particle states that are to be considered as part of the vapor and from those that are part of the “nucleus” by use of the reflection and transmission coefficients, as discussed in Section 2. It should be noted that the result (15) is exactly what would have resulted from considering a Fermi gas confined strictly within the well, *i.e.* by putting $R_0 = R$.

For the following discussion, a general (unbound) orbital is denoted a *global* orbital, since it satisfies the condition of phase match (2) relevant to the entire container. As the energy is gradually raised, there will occasionally be a local phase match, *i.e.* the phase accumulated from the origin to the boundary of the well is a multiple of π , $kR = n\pi$. Such orbitals shall be referred to as *local*. (Generally, local and global matches will *not* occur simultaneously, but this is unimportant for our present discussion; one may, for example, identify the local orbital as that global orbital which has the best local match.) By comparing the global and local matching conditions, it is readily seen that

$$\frac{dN}{dn} = \left[\frac{R_0 - R}{k_0} + \frac{R}{k} \right] \frac{k}{R} \approx \frac{R_0}{R} \frac{k}{k_0} \quad (16)$$

Here the last relation holds when $R_0 \gg R$ and in that case there is a local state for each k/k_0 global states. In a given energy interval $d\epsilon$ there are $dN = g(\epsilon)d\epsilon$ global states and of these

$$dn = \frac{dn}{dN} dN = \frac{R}{k} \left[\frac{R_0 - R}{k_0} + \frac{R}{k} \right]^{-1} \frac{m}{\pi \hbar^2} \left[\frac{R_0 - R}{k_0} + \frac{R}{k} \right] d\epsilon = \frac{m}{\pi \hbar^2} \frac{R}{k} d\epsilon \quad (17)$$

are then also local states. This is the exact same number as what would result if we were instead to artificially confine the well (*i.e.* put $R_0 = R$), since in that case the number of states contained within the same energy interval would be $g_{<}(\epsilon)d\epsilon = (m/\pi \hbar^2)(R/k)d\epsilon$. This result shows that considering those global states that are also local is equivalent to considering all the states in the artificially confined well. (Only those states with $\epsilon > 0$ should be considered, of course, or alternatively, the class of local states should be redefined so as to include also the bound states.)

The above analyzes serve to illustrate how the various points of view regarding the problem are mutually consistent. For simplicity, we have relied on semiclassical considerations. In a more rigorous treatment the orbitals should be represented by standing waves of the form (6). The matching conditions are then transcendental and the resulting formulae are less transparent. However, the qualitative features remain the same.

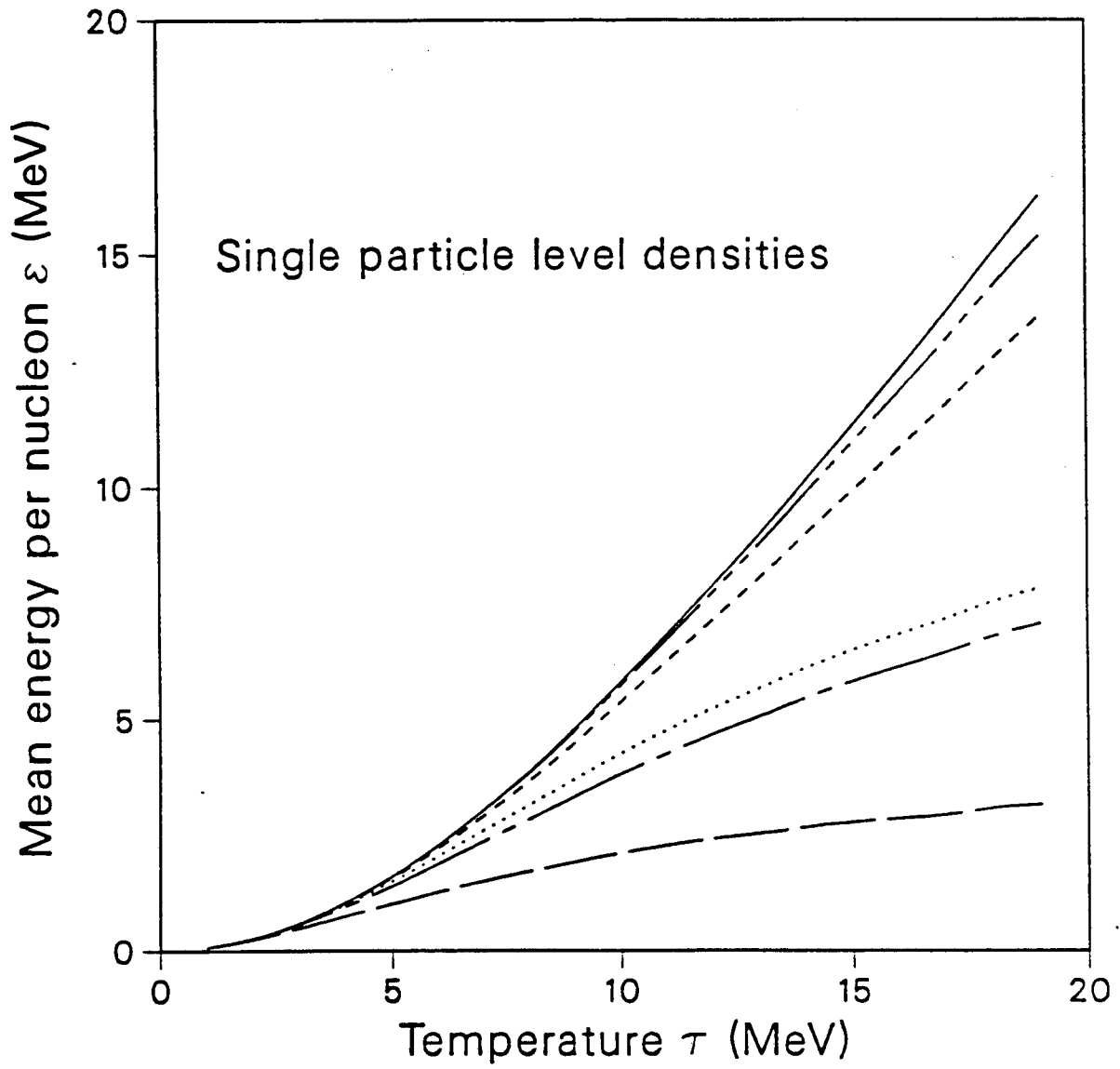
References

- [1] A.Z. Mekjian, Phys. Rev. Lett. **38**, 640 (1977).
- [2] J. Gosset, J.I. Kapusta, and G.D. Westfall, Phys. Rev. **C18**, 844 (1978).
- [3] S.E. Koonin and J. Randrup, Nucl. Phys. **A356**, 223 (1981).
- [4] W.A. Friedman and W.G. Lynch, Phys. Rev. **C28**, 16 (1983); Phys. Rev. **C28**, 950 (1983).
- [5] L.G. Moretto and G.J. Wozniak, preprint, LBL-24558 (1987).
- [6] L.G. Moretto, Nucl. Phys. **A247**, 211 (1975).
- [7] G. Fai and J. Randrup, Nucl. Phys. **A381**, 557 (1982).
- [8] G. Fai and J. Randrup, Nucl. Phys. **A404**, 551 (1983).
- [9] S.E. Koonin and J. Randrup, Nucl. Phys. **A474**, 183 (1987).
- [10] J. Pochodzalla *et al.*, Phys. Rev. Lett. **55**, 177 (1985).
- [11] Z. Chen *et al.* Phys. Rev. **C36**, 2297 (1987).
- [12] G. Fai and J. Randrup, Comp. Phys. Comm. **42**, 385 (1986).
- [13] G.F. Bertsch, H. Kruse, and S. DasGupta, Phys. Rev. **C29**, 673 (1984).
- [14] H. Kruse, B.V. Jacak, and H. Stöcker, Phys. Rev. Lett. **54**, 289 (1985).
- [15] C. Gale, G.F. Bertsch, and S. Das Gupta, Phys. Rev. **C35**, 1666 (1987).
- [16] J. Aichelin, A. Rosenhauer, G. Peilert, H. Stöcker, and W. Greiner, Phys. Rev. Lett. **58**, 1926 (1987).
- [17] D.L. Tubbs and S.E. Koonin, Astrophys. J. **232**, L59 (1979).
- [18] D.Q. Lamb, J.M. Lattimer, C.J. Petchik and D.G. Ravenhall, Nucl. Phys. **A432**, 646 (1985).
- [19] E. Suraud, P. Schuck, and R.W. Hasse, Phys. Lett. **164B**, 212 (1985).
- [20] D.R. Dean and U. Mosel, Z. Phys. **A322**, 647 (1985).
- [21] H.A. Weidenmüller, Ann. Phys. **28**, 60 (1964).
- [22] G. Fai, L.P. Csernai, J. Randrup, and H. Stöcker, Phys. Lett. **164B**, 265 (1985).
- [23] L.P. Csernai, G. Fai, J. Randrup, and L. Sathpathi, in preparation.

- [24] T.J. Mazurek, J.M. Lattimer, and G.E. Brown, *Astrophys. J.* **229**, 713 (1979).
- [25] P. Bonche, S. Levit, and D. Vautherin, *Nucl. Phys.* **A427**, 278 (1984).
- [26] M.S. Sano and S. Yamasaki, *Progr. Theor. Phys.* **29**, 397 (1963).
- [27] A. Bohr and B.R. Mottelson, *Nuclear Structure*, Vol. 1. W.A. Benjamin, New York (1969).
- [28] S. Pratt, P. Siemens, and Q.N. Usmani, *Phys. Lett.* **189B**, 1 (1987).
- [29] N. Levinson, *Kgl. Danske Videnskab. Selskab.* **25**, 9 (1949).
- [30] B.R. Mottelson, *Proceedings of the Niels Bohr Centennial Conference on Nuclear Structure*, Copenhagen, 20-24 May (1985) 3.
- [31] P. Bonche, D. Vautherin, and M. Vénéroni, *J. de Physique*, **C4**, 339 (1986).
- [32] N. Fröman and P.O. Fröman, *JWKB Approximation*, North-Holland, Amsterdam (1965).
- [33] W.D. Myers, *Nucl. Phys.* **A145**, 387 (1970).
- [34] L.D. Landau and E.M. Lifshitz, *Quantum Mechanics*, Pergamon Press (1965).
- [35] M.A. Preston, *Physics of the Nucleus*, Addison-Wesley (1965).
- [36] J. Tōke and W.J. Świątecki, *Nucl. Phys.* **A372**, 141 (1981).
- [37] R.W. Hasse and P. Schuck, *Nucl. Phys.* **A445**, 205 (1985); preprint, GSI-86-20 (1986).
- [38] P.F. Bortignon and C.H. Dasso, *Phys. Lett.* **189B**, 381 (1987).
- [39] M.K. Grossjean and H. Feldmeier, *Nucl. Phys.* **A444** 113, (1985).
- [40] C.J. Pethick and D.G. Ravenhall, preprint, ILL-(TH)-87-#28 (1987).
- [41] W.A. Friedman, preprint, Mad/NT/88-01 (1988).

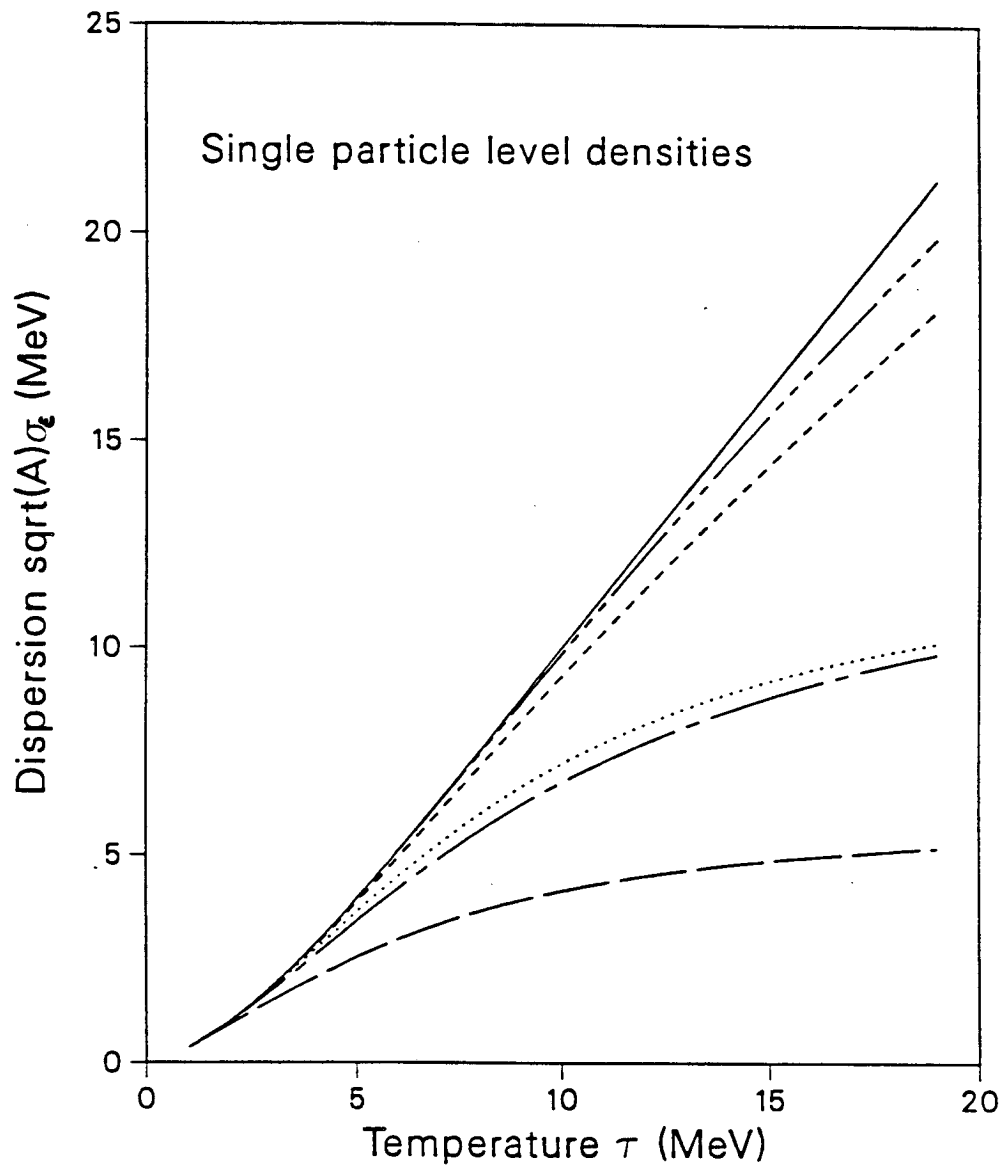
Figure Captions

- Fig. 1:** The mean excitation energy per nucleon in a quasifragment \mathcal{E} , as given by (13) (a), and the square root of the reduced variance (14) (b), as functions of the imposed temperature τ , for the hot and cool scenarios (full curve and long dashes, respectively), with an exponential cut-off (17) (using widths τ_0 of 100 MeV and 12 MeV, short dashes and dash-dots, respectively), and with a gaussian cutoff (18) (again, using 100 MeV and 12 MeV for the width, alternating long-short dashes and dotted line, respectively). The plotted quantities are independent of the mass number A .
- Fig. 2:** Mean energy per nucleon in a quasifragment \mathcal{E} , as given by (13) as a function of the imposed temperature τ , for the hot and cool scenarios (full curve and long dashes, respectively), and with various modulating factors. Modulating the Fermi-gas level density with the average reflection coefficient $\bar{R}_A(\epsilon)$ yields the dashed and dotted curves, corresponding to $A = 40$ and $A = 100$, respectively. The results of the exponential modulation using a width of 12 MeV are included from the previous figure for comparison. The dash-dotted curve corresponds to using the reflection coefficient appropriate to a diffuse, flat potential (for which the centrifugal force is ignored).
- Fig. 3:** Mean energy per nucleon in a quasifragment \mathcal{E} (a), and the square root of the reduced variance as given by (14) (b), as functions of the imposed temperature τ , calculated on the basis of the many-body level density (27) in the saddle-point approximation for $A = 20$ (dots), $A = 40$ (short dashes), and $A = 100$ (long dashes). The results of the calculation with the hot scenario based on the single-particle level density is included for comparison (full line).
- Fig. 4:** Mean energy per nucleon in a quasifragment \mathcal{E} as a function of the imposed temperature τ , calculated with the level densities (29) and (30). Short dashes and long dashes represent the results of the calculation using (29) with $e_0 = 8, 16$ MeV, respectively. Alternating long-short dashes and the dotted line correspond to (30) with $e_0 = 8, 16$ MeV, respectively. The result of the full calculation based on the Fermi-gas single-particle level density is included for comparison (solid line).
- Fig. 5:** Mean energy per nucleon in a quasifragment \mathcal{E} as a function of the imposed temperature τ for $A = 40$, calculated on the basis of ref. [36], with several values of the parameters, as explained in the text.
- Fig. 6:** Total mean excitation energy in quasifragments as a function of the mass number A for the disassembly of a source with total mass and charge $A_0 = 40, Z_0 = 20$, and excitation energy $\epsilon = 20$ MeV, with different modulating factors. The darkest vertical bars in the foreground represent the standard (mass-dependent) Gaussian cutoff (see text), used in the *FREESCO* event generator and fitted to available data. The second and the third bars correspond to exponential cutoffs with $e_0 = 8, 16$ MeV, respectively.



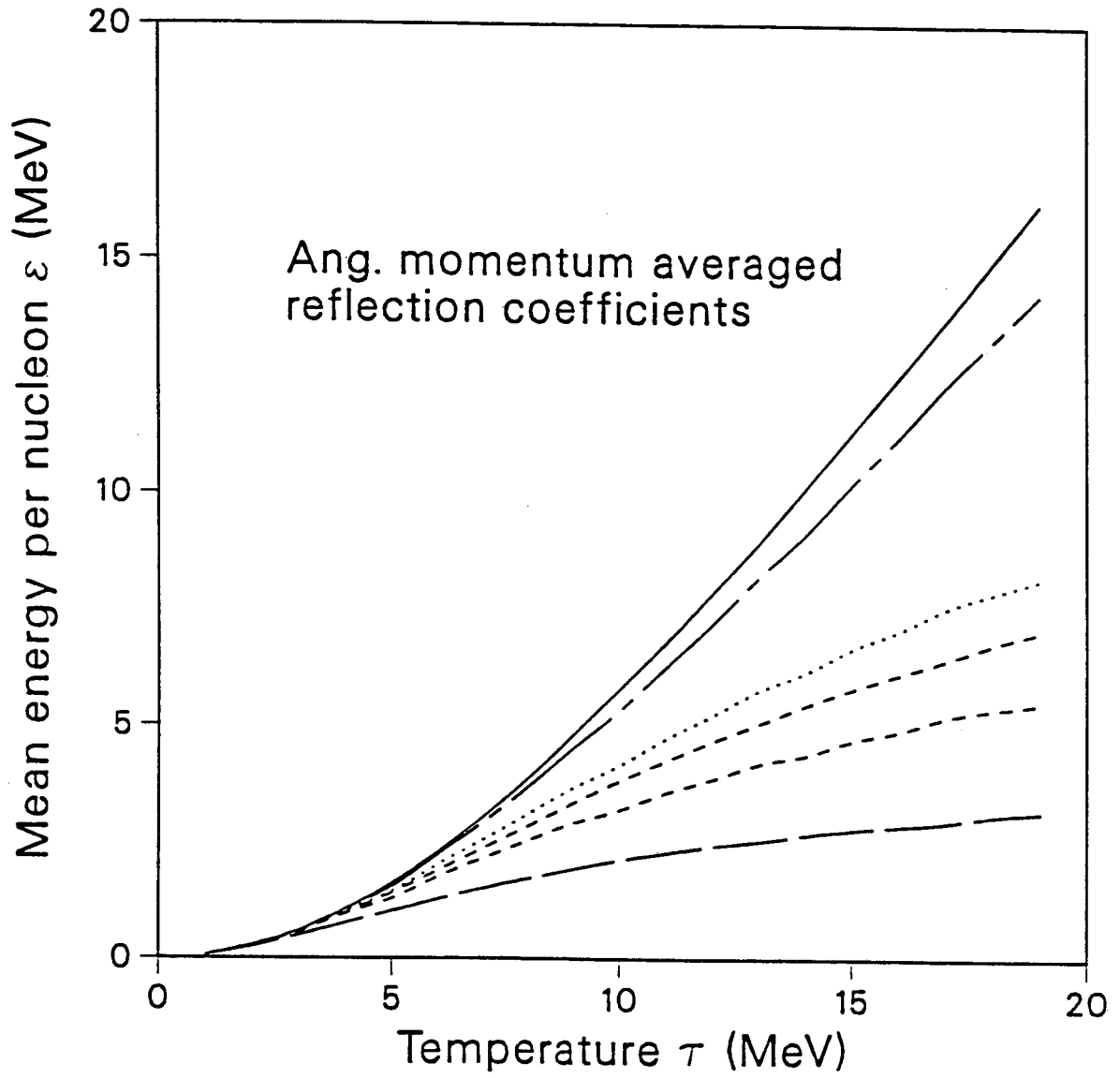
XBL 883-946

Figure 1a



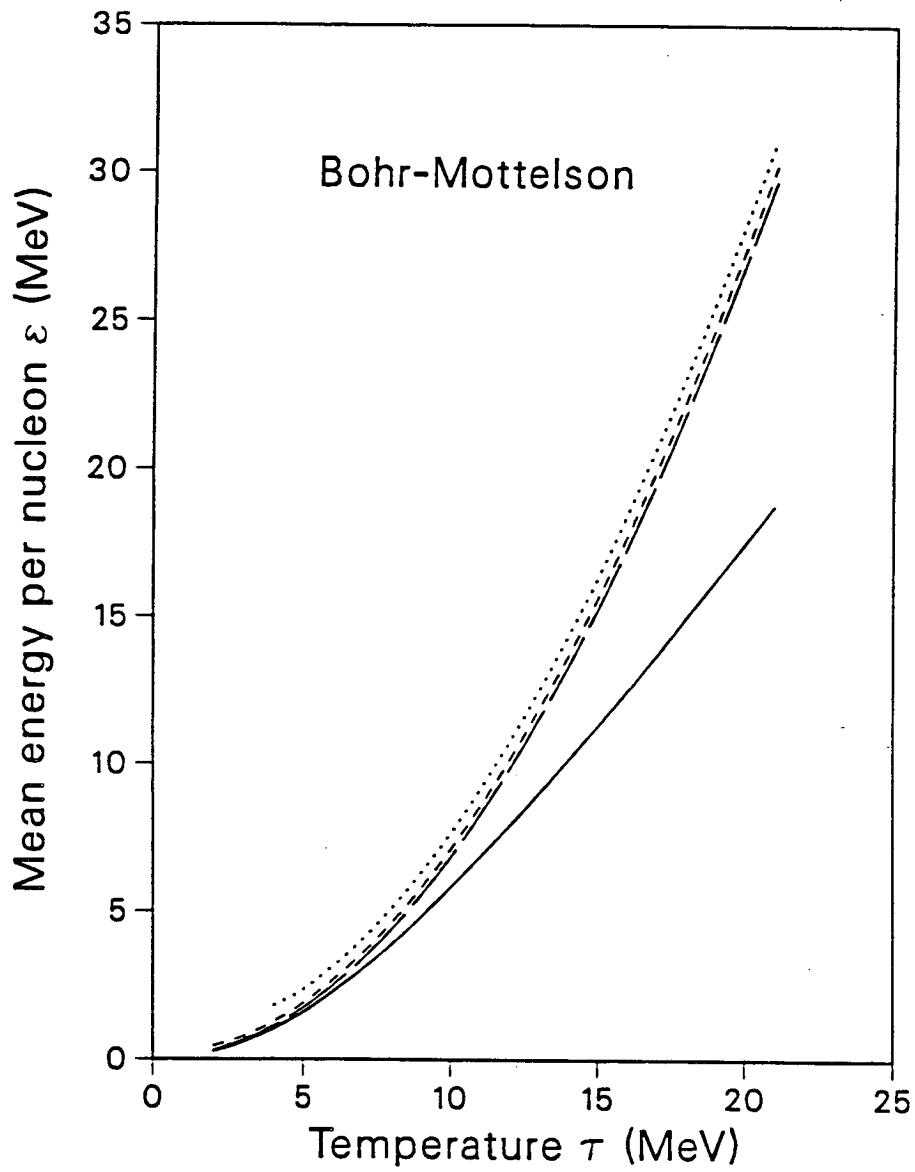
XBL 883-947

Figure 1b



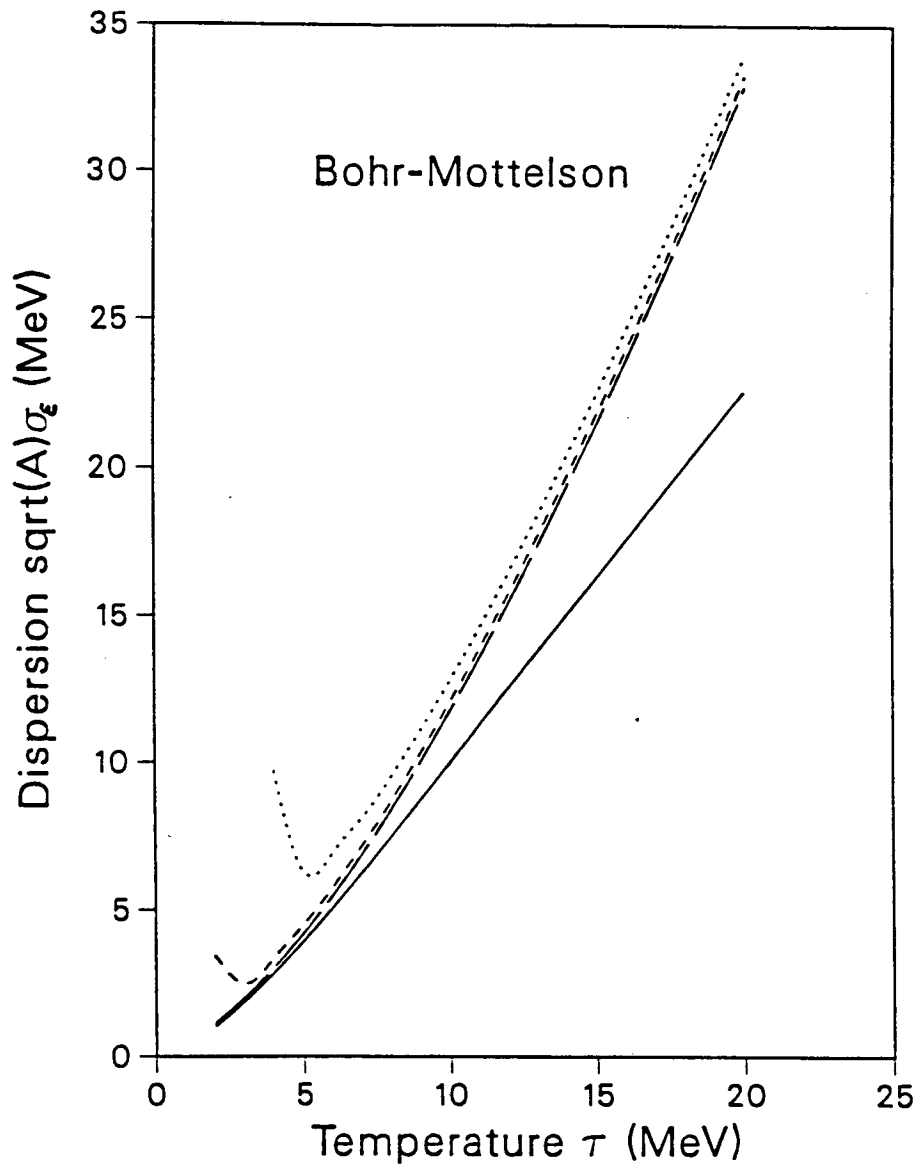
XBL 883-948

Figure 2



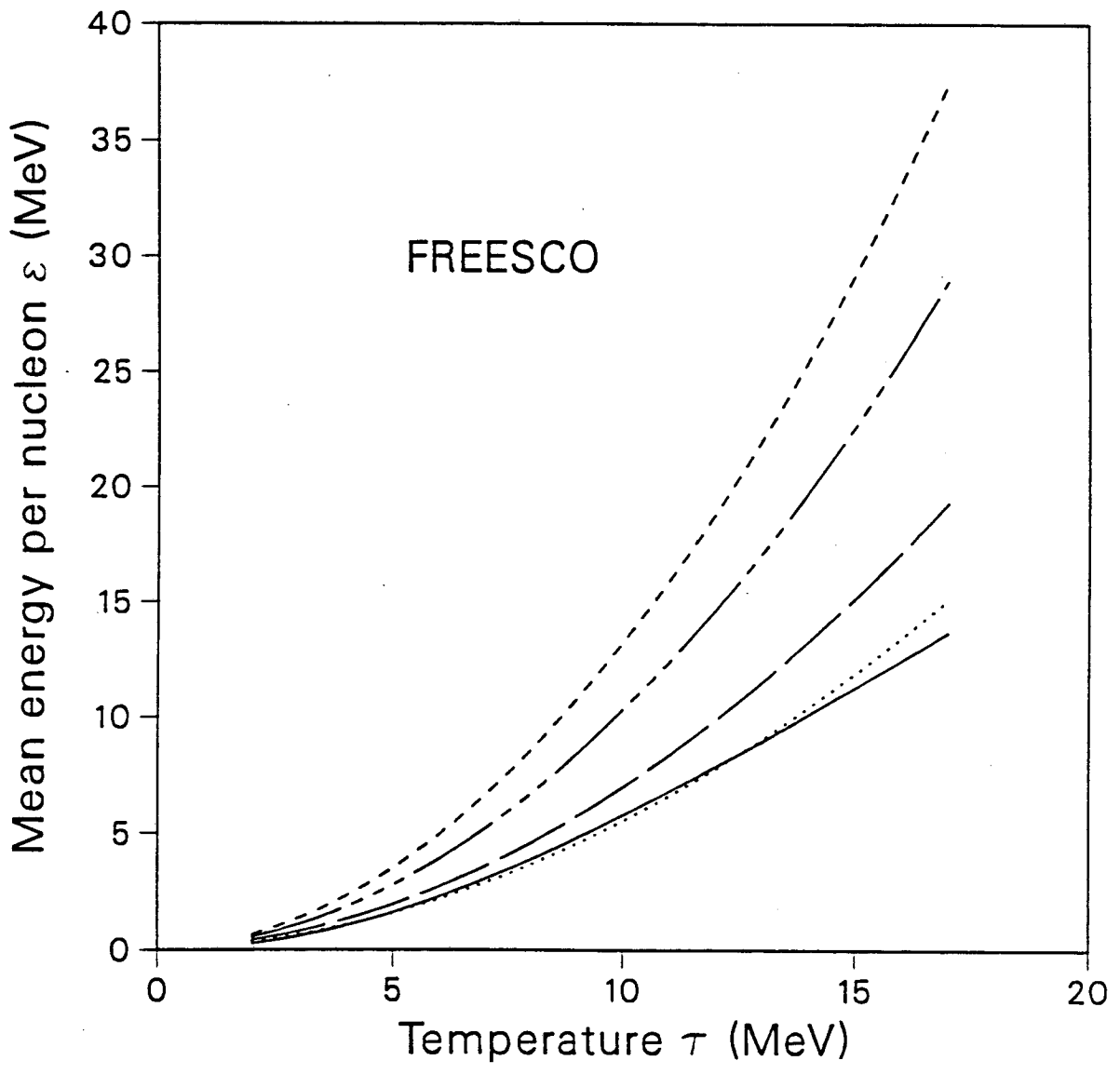
XBL 883-950

Figure 3a



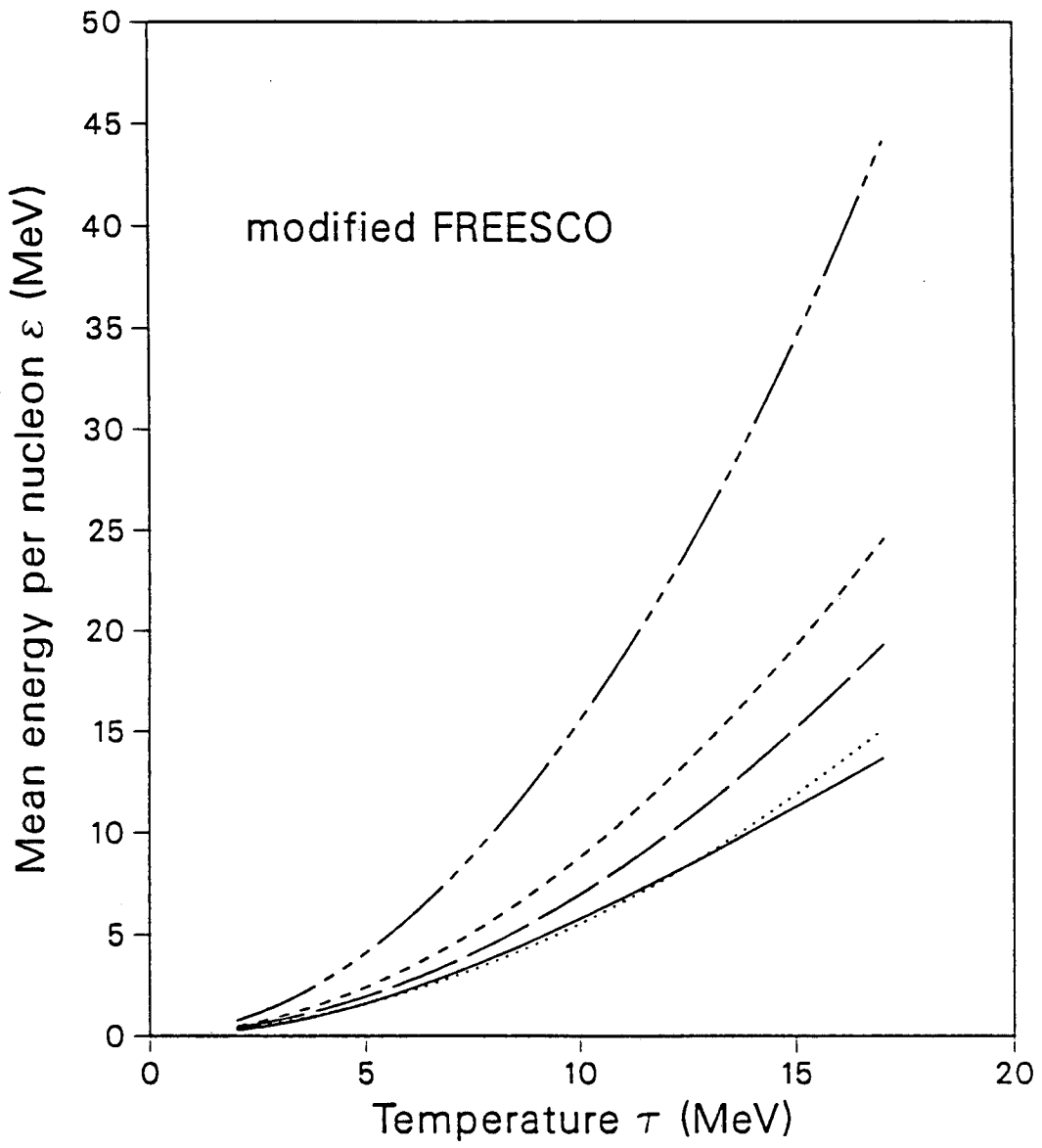
XBL 883-951

Figure 3b
25



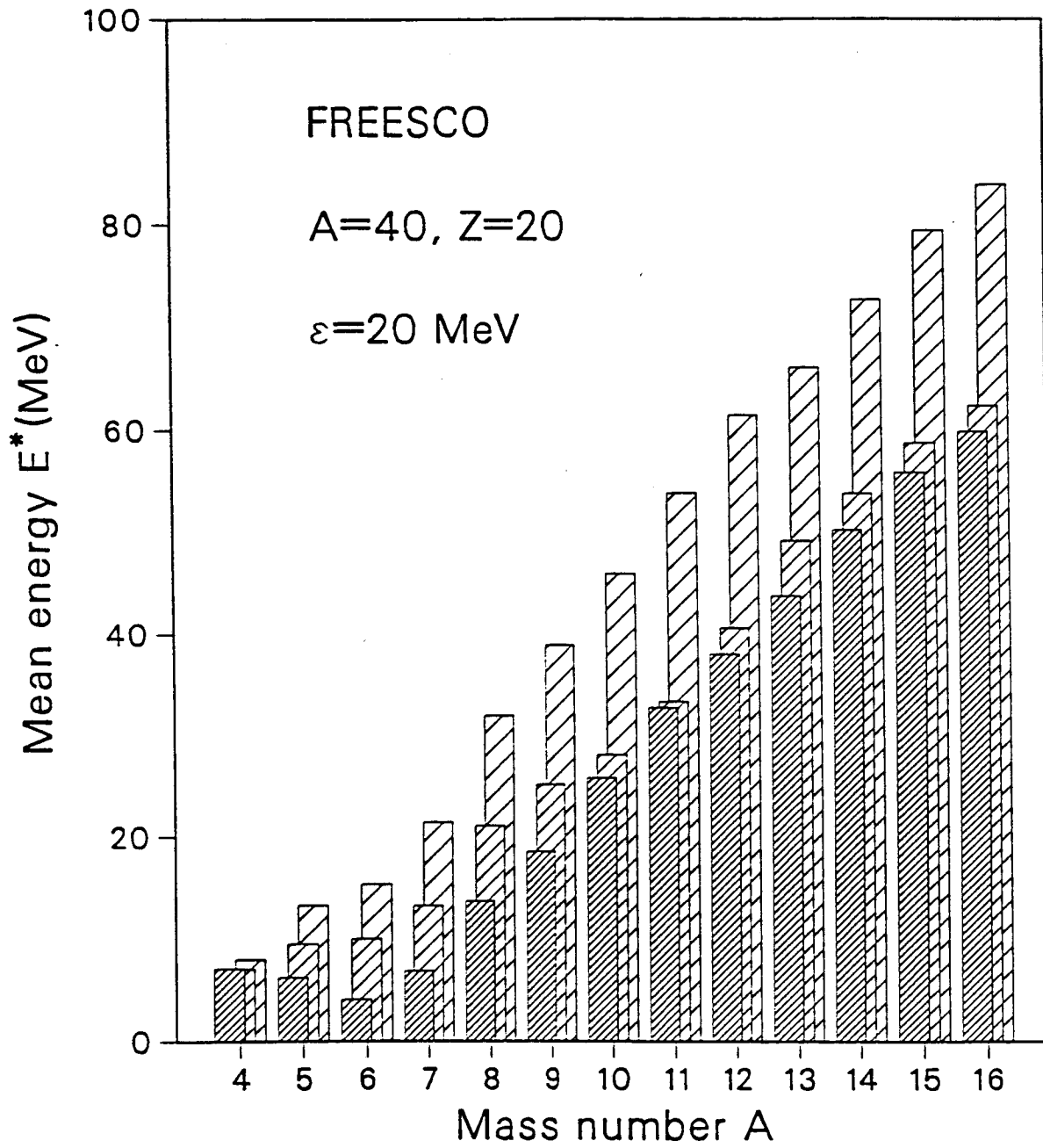
XBL 883-952

Figure 4



XBL 883-955

Figure 5



XBL 883-956

Figure 6
28

LAWRENCE BERKELEY LABORATORY
TECHNICAL INFORMATION DEPARTMENT
UNIVERSITY OF CALIFORNIA
BERKELEY, CALIFORNIA 94720